J. Electron Microsc., Vol. 28, No. 1, 1-11, 1979

Development of a Field Emission Electron Microscope

Akira TONOMURA, Tsuyoshi MATSUDA, Junji ENDO,
Hideo TODOKORO and Tsutomu KOMODA

Central Research Laboratory, Hitachi Ltd., Kokubunji, Tokyo, 185 Japan

(Received August 1, 1978; accepted December 25, 1978)

A field emission electron microscope with highly stabilized gun and illuminating system was developed. Several experiments were made to demonstrate the high performance of the microscope. The brightness of the beam was more than that of the conventional ones, which feature was demonstrated by taking 300 Fresnel fringes and 3,000 bi-prism fringes. Furthermore, monochromatic feature of the microscope makes the effect of chromatic aberration smaller and the half-spacing fringes of nickel {220} planes (1/2 d_{220}=0.62 Å) were observed.

***Key words*=field emission: coherence: lattice resolution: electron bi-prism: electron holography**

INTRODUCTION

The ultimate purpose of high resolution electron microscopy lies in observing various kinds of natural phenomena with a measure of atoms and molecules. For that purpose, improvement of the resolution is still required. The resolution of an electron microscope was restricted by fundamental limitations, that is, aberrations of the electron lenses. Meanwhile, subsidiary conditions, such as stabilities of power supplies and mechanics, have been greatly improved for the last ten years, and so the fundamental effect of lens aberrations appear clearly in high resolution images.

In order to remove these image defects proper to an electron microscope, a number of innovative researches and developments have been made.[1] However, means to overcome the present standstill are not found, up to this time.

We have developed a field emission electron microscope as a tool to break the difficulty. The field emission electron beam has a monochromatic feature, which can make the chromatic aberration smaller and which can improve the resolution of an electron microscope. Another feature of the coherent beam makes the phase contrast of an image higher. In addition, the latter also makes it possible to correct the spherical aberration of an electron lens by realizing electron holography.[2-4]

Field emission electron microscopes so far developed have not made a direct contribution to the performance of an electron microscope. This may be due to the fact that the current density of illuminating beam onto a specimen was not large enough to observe a high resolution image and also that the illuminating beam is not so highly stabilized as to realize coherent illumination.

Several experiments have been made to confirm that the apparatus has a potential to reach the above-mentioned purpose.

CONSTRUCTION OF FIELD EMISSION ELECTRON MICROSCOPE

Figure 1 shows an outside view of our field emission electron microscope. The column below the objective lens is that of Hitachi HU-12A electron microscope. The gun, the illuminating system and the specimen chamber were designed to be magnetically shielded from outer disturbances. An electron bi-prism is installed in a field-limiting aperture plane in order to investigate the spatial coherency of

Fig. 1. Outside view of field emission electron microscope.

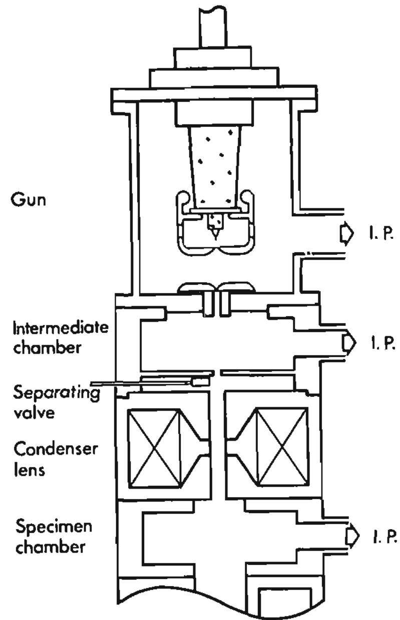

Fig. 2. Cross-sectional diagram of gun and illuminating system.

the beam. Each part is in detail described below.

1. Gun and illuminating system

A cross-sectional diagram of the gun and the illuminating system are shown in Fig. 2. Electrons were emitted from ⟨310⟩-oriented tungsten tip by applying a potential of 3–6 kV between the tip and the first anode. The total emission current was usually 100 μA. About one percent of the electrons is passed through the aperture of the first anode and then is accelerated by Butler type anodes. The shape of the anodes was designed to minimize the spherical aberration of the accelerating electrostatic lens. Far below the specimen plane, the real image of the electron source was formed by the accelerating lens. The diameter of the spot formed on a specimen plane is 300 Å. In general, electrons are not focused on a specimen plane, but are a little defocused to illuminate a larger area. The accelerating voltage was 70 kV in the present experiment. The gun was able to be operated for more than three hours without thermally flashing the tip.

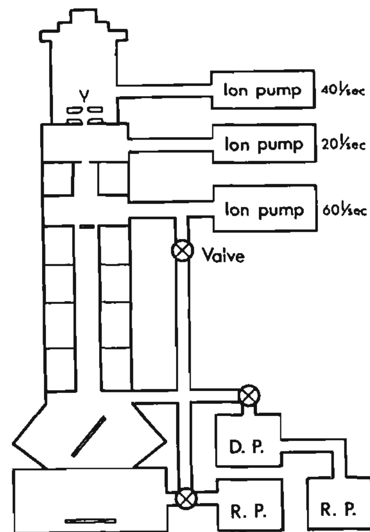

Fig. 3. Evacuating system of field emission electron microscope.

2. Evacuating system

The gun chamber was evacuated by two 20 *l*/s ion pumps (See Fig. 3). An intermediate chamber is situated for differential pumping between the gun and a condenser lens and is also evacuated by a 20 *l*/s ion pump. Specimen chamber is evacuated by a 60 *l*/s ion pump. The final pressures in gun, intermediate and specimen chambers are 5×10^{-10}, 1×10^{-9}, and 1×10^{-6} Torr, respectively.

3. Interferometer of electron bi-prism

A Möllenstedt type electron bi-prism[5,6] is installed on the field-limiting aperture plane[7] to investigate the coherent characteristics of the electron beam. Figure 4 shows a perspective drawing of an electron bi-prism. The bi-prism wire was made of 0.3 μm^{ϕ} quartz fiber, on which gold was evaporated. The fiber was placed between two parallel plates of earth potential. A potential of 0~200 V was applied through a spring lead from outside a vacuum. The bi-prism was movable in a plane perpendicular to the direction of electron-beam trajectory, which mechanism was the same as that of the field-limiting aperture.

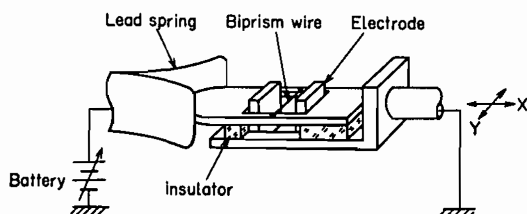

Fig. 4. Perspective drawing of electron bi-prism.

PERFORMANCE CHARACTERISTICS

The high brightness of a field emission electron beam realizes coherent illumination in an electron microscope. Therefore, the amount of the brightness was estimated backward from the interference experiments. Then, lattice images were taken to investigate the decreased effect of chromatic aberration due to the narrow energy spread of the beam.

1. Estimation of the beam brightness

Fresnel fringes were employed to estimate the brightness of the field emission electron beam. The formation of Fresnel fringes is illustrated in Fig. 5. Nearly plane wave with a divergent angle of 2β illuminates the edge of a specimen. The transmitted wave and the diffracted waves from the edge interfere with each other on a observation plane and then they form Fresnel fringes. The spacing of the fringes becomes smaller with the distance from the edge. The minimum spacing is limited by the diameter of an illumination cone on the observation plane (See Fig. 5).

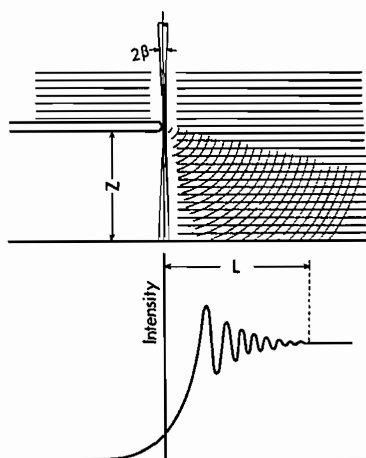

Fig. 5. Schematic diagram of Fresnel fringes. Nearly plane wave illuminates an edge of a specimen and the interference fringes between the plane wave and the diffracted wave from the edge are observed. The illumination angle 2β limits the minimum fringes observable.

The length of the region where *n* fringes appear is given by

$$L \sim \sqrt{2n\lambda Z} \quad (1)$$

where Z is the distance between the specimen and observation planes and λ is the wavelength of electrons.

In order to obtain the coherent region as large as the length L, the illumination angle 2β ought to be as small as $2\beta < \lambda/L$.

Meanwhile, when photographing the fringes, the fringe with the minimum spacing should be

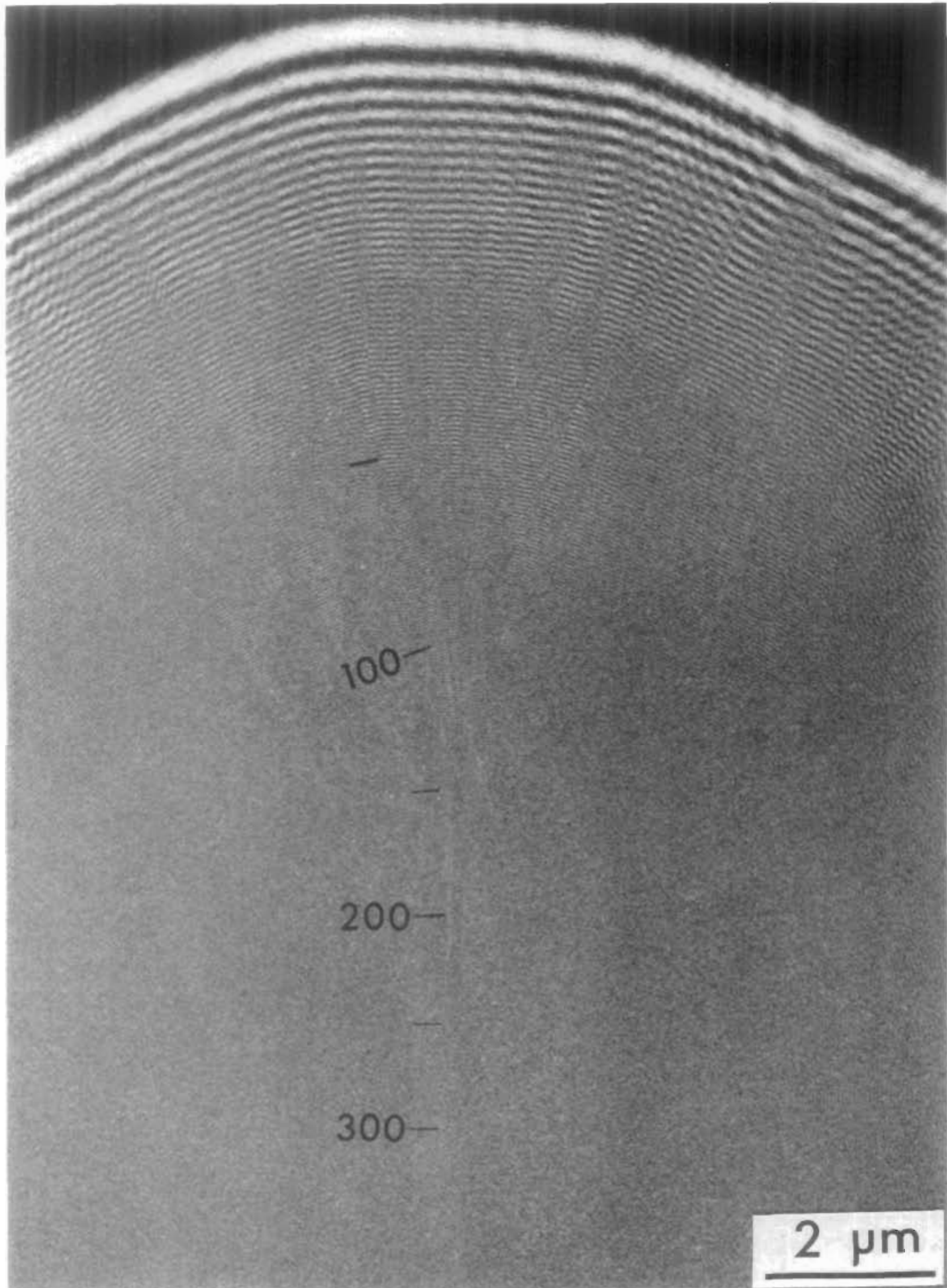

Fig. 6. Fresnel fringes from a microgrid edge. The number of the fringes is 300, which is the largest among those reported to date.

exposed with moderate exposure time to record on film. This condition requires large illumination angle 2β.

Therefore, the illumination angle has the optimum value to obtain the largest fringe number. The maximum number for the optimum condition is given by

$$n_{\max}=\frac{\lambda}{4d\sqrt{\frac{I}{B\pi T}}} \quad (2)$$

where B is beam brightness, T exposure time, I the amount of charge density necessary to expose a film and d the resolution of the film.

As λ, d and I are constant, $n_{\max}$ depends only on B and T. Therefore, beam brightness can be estimated from the maximum number of fringes obtained. Fresnel fringes from a microgrid edge taken with the field emission electron microscope are shown in Fig. 6. The amount of defocus Z is 8 mm, the magnification m is 1,300, and the exposure time is only 4 s. The 300 Fresnel fringes are observed. The number of these fringes is the largest among those reported to date. According to Eq. (2), the resultant brightness is estimated to be 2×10^{8} A/cm$^{2}\cdot$sr, when $I=5\times10^{-11}C/\text{cm}^{2}$ and $d=30\ \mu$m. This result shows that the beam brightness is 100 times larger than that of thermionic electron beam, and that the coherent illumination becomes possible in the microscope, and that the phase contrast will be very high even in highly defocused images, which is the case with biological specimens.

Owing to the high brightness of the electron beam, much more bi-prism fringes are expected to be obtained than hitherto reported. From our experiments, 3,000 bi-prism fringes could be observed with our microscope using a Möllenstedt type bi-prism.[8] The fringes are shown in Fig. 7 (a). Only a part of the pattern is enlarged in Fig. 7 (b). The maximum number of fringes that have been taken is at most 300. Therefore, this result corresponds to the improvement of spatial coherence length by ten times. As an application of this technique, experiments of electron holography were carried out. An off-axis hologram was formed by the interference between object and reference waves, which was produced by the electron bi-prism. The image hologram of an evaporated gold particle is shown in Fig. 8. The exposure time required was 8 s. The magnification of the hologram was 140,000 times. A potential of 100 V was applied to the bi-prism wire. When an image is exactly focused, Bragg-reflected waves from {111} planes are formed outside the image, due to the spherical aberration of the electron lens ($C_s=1.7$ mm). Inside the Bragg-reflected images, interference fringes between the reflected and transmitted waves are faintly observed. Furthermore, the oblique interference fringes between the reflected and the reference waves are also observed there. The hologram was illuminated with a He-Ne laser light and then the reconstructed image was obtained under any focusing condition. The exact focused reconstructed image is shown in Fig. 9. Lattice image is reconstructed outside the particle. This shows that the Bragg-reflected waves from {111} planes are certainly reconstructed, and that the lattice resolution of the image reconstructed is better than 2.4 Å.

2. Improvement of lattive resolution

Monochromatic feature of the field emission electron beam is expected to improve the lattice resolution of an electron microscope, because the lattice resolution limit has been restricted by the chromatic aberration. In order to show this, the effect of the field emission electron beam on lattice imaging was investigated. In general, there are three methods of lattice imaging, that is, axial two-wave interference, axial three-wave interference and titled two-wave interference. The schematic diagram for the former two methods is shown in Fig. 10. In the following, the contrast of lattice image is discussed with respect to chromatic aberration in each case.

1) The method of axial two-wave interference. The contrast of normal lattice fringes formed in this method is decreased by the

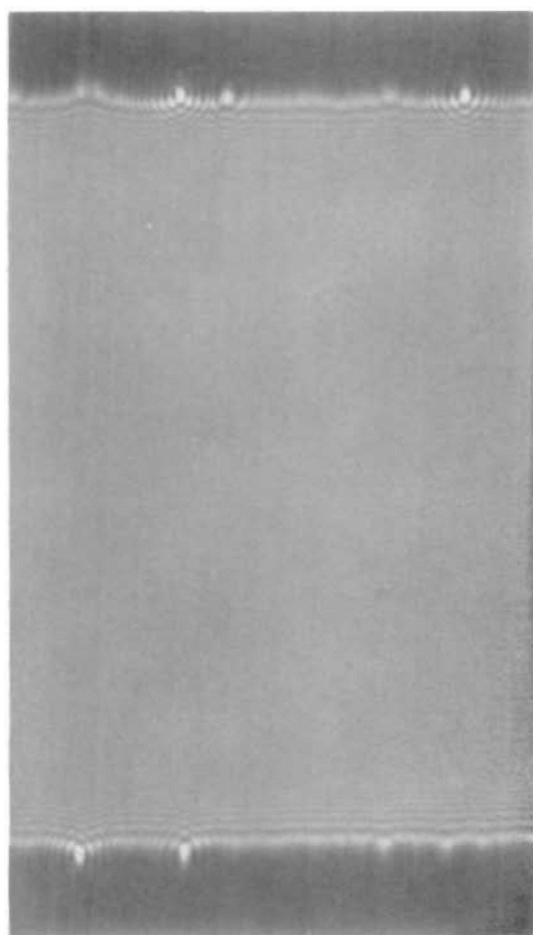

(a)

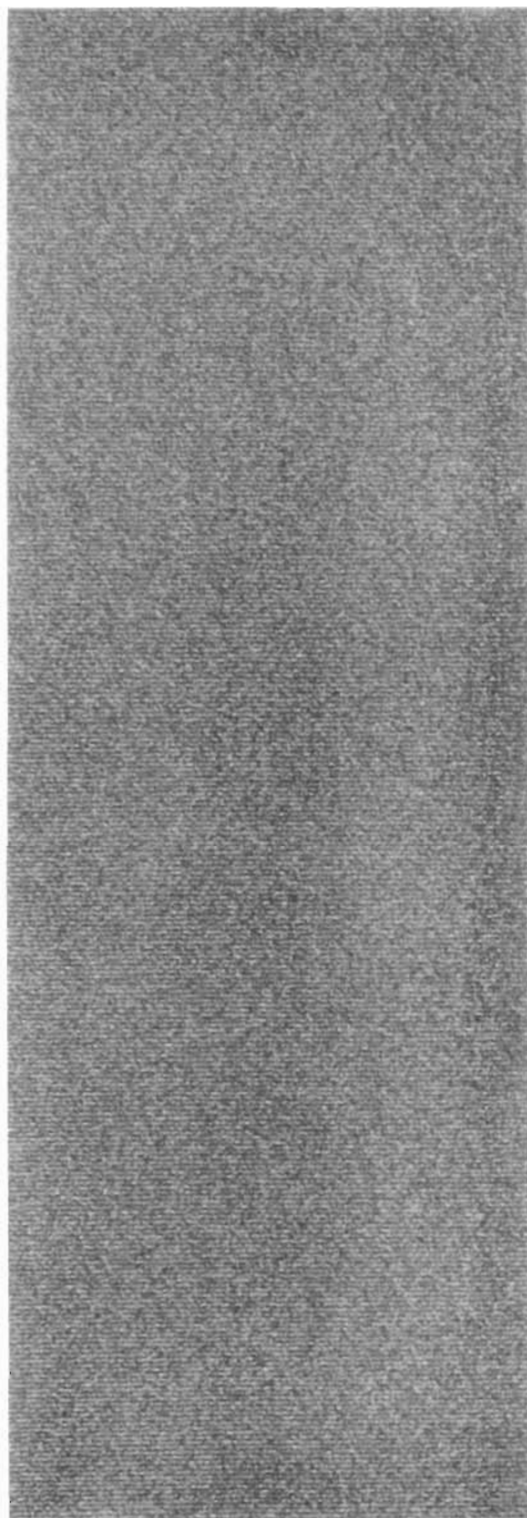

(b)

Fig. 7. Interference fringes produced by a Möllenstedt type bi-prism. The number is 3,000, which is 10 times larger than those reported to date. (a) The whole interference pattern. (b) The enlarged interference fringes.

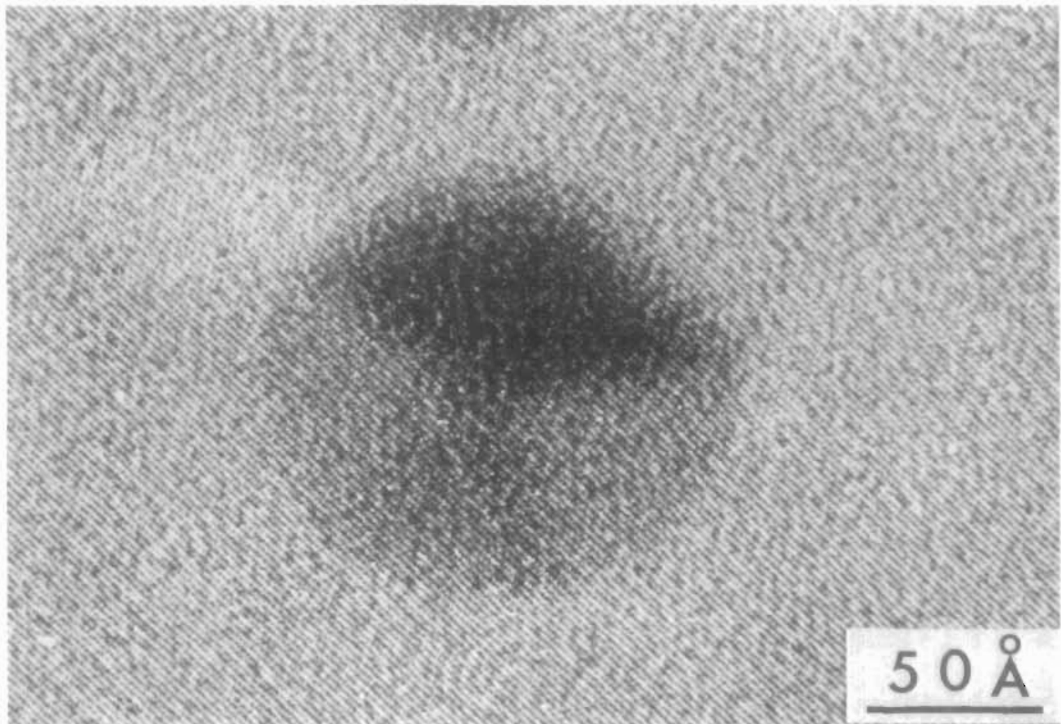

Fig. 8. Image hologram of an evaporated gold particle. In addition to bi-prism and lattice fringes, oblique interference fringes between the reference wave and the Bragg-reflected waves are observed where the reflected images are located.

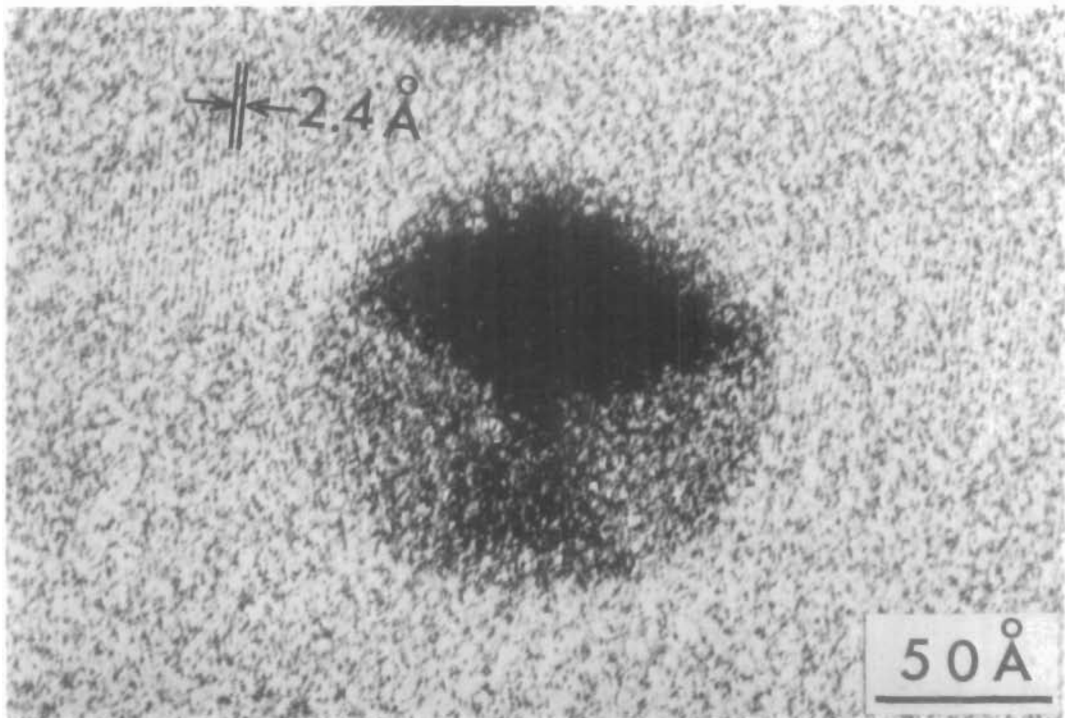

Fig. 9. Reconstructed image of a gold particle. The defocused lattice image is observed outside the particle. This shows that the resolution of the reconstructed image is 2.4 Å.

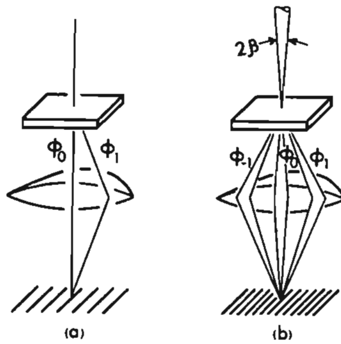

Fig. 10. Schematic diagram of lattice imaging. (a) Axial two-wave interference. (b) Axial three-wave interference.

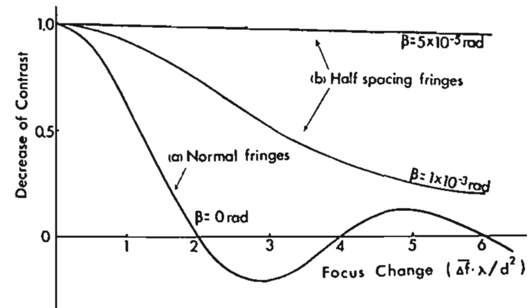

Fig. 11. Decrease of lattice image contrast due to the chromatic aberration. The value in the ordinate is so normalized that it is 1.0 in the case of no chromatic aberration $(\overline{\Delta f}=0)$. The negative value means the inversion of the fringe contrast.

chromatic defect of an electron lens. The energy change of electrons, which is related to the defocusing, makes the lattice fringes move laterally. The contrast of lattice fringes decreases by overlapping the fringes shifted variously. Due to this effect, the contrast decreases sensitively by the instability of high voltage and lens current, and by the energy spread of electron beam. The decrease of the contrast is estimated under the condition of the uniformed energy distribution corresponding to the defocusing width $\overline{\Delta f}$ to be[9] $\{\sin(\pi\lambda\overline{\Delta f}/2d^2)\}/(\pi\lambda\overline{\Delta f}/2d^2)$. It is plotted against $(\overline{\Delta f}\cdot\lambda/d^2)$ in Fig. 11, where d is the lattice spacing considered. It seems reasonable to assume that lattice fringes are resolved when the contrast of fringes is more than 64%,

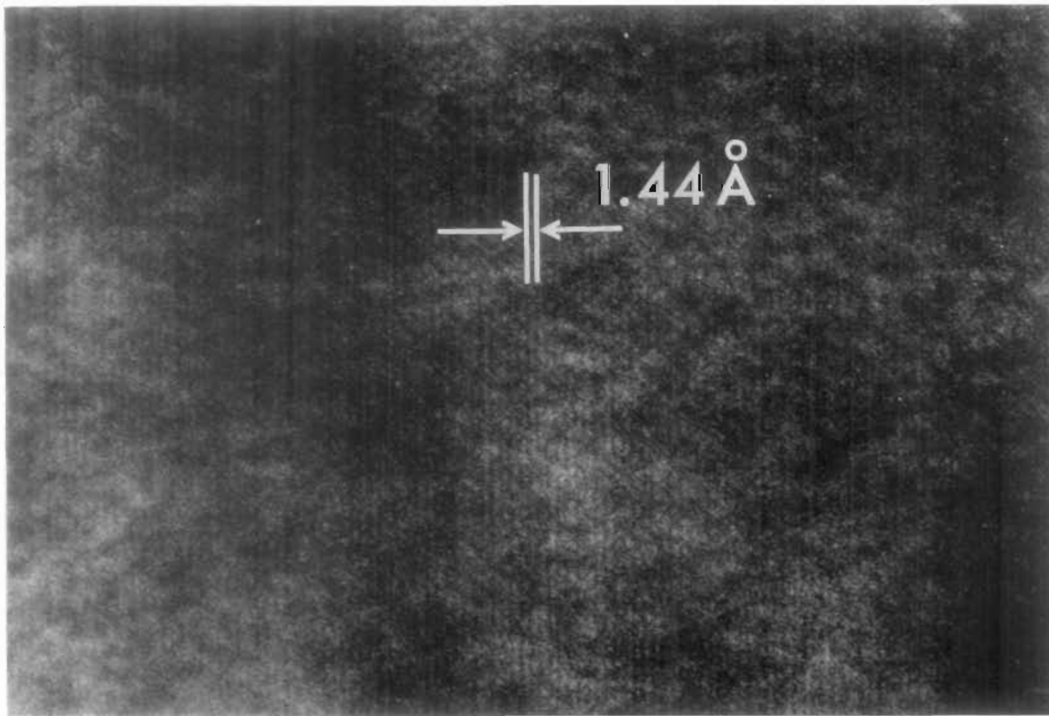

Fig. 12. Lattice fringes of gold {220} planes formed by the axial two-wave interference. The spacing of 1.4 Å is clearly resolved.

which condition corresponds to $(\pi\lambda\overline{\Delta f}/2d^2)=(\pi/2)$. The lattice resolution can be obtained as

$$d=\sqrt{\overline{\Delta f}\cdot\lambda}=\sqrt{C_c\lambda\frac{\Delta E}{E}},$$

where C_c is the coefficient of the chromatic aberration and $\Delta E/E$ is the variation of the electron energy, consisting of the instability of high voltage and lens current, and the energy spread of the electron beam. As the power stability of the apparatus (high voltage and lens current) is better than 2×10^{-6}/min and the energy spreads of electrons from thermionic hairpin and pointed filaments are about 2 and 1 eV, respectively, $\Delta E/E$ is mainly determined by the latter. When $C_c=1.5$ mm and $E=70$ kV, these lattice resolutions become 4 and 3 Å, respectively. Lattice resolution was actually improved using pointed filaments.[10]

Meanwhile, the reported energy spread of field emission electrons is 0.2~0.4 eV and therefore the line resolution taken with the axial illumination is expected to be 1.3~1.9 Å. Actually gold {220} lattice fringes ($d_{220}=1.4$ Å) formed by the axial two-wave interference were clearly resolved with the present microscope as shown in Fig. 12. This result shows that the effect of chromatic aberration decreases with the new microscope and that the lattice resolution becomes higher.

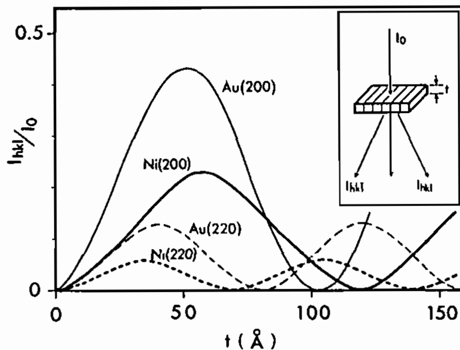

Fig. 13. Calculated intensities of simultaneous Bragg-reflections by three-wave approximation.

2) The method of axial three-wave interference. In addition to the normal lattice fringes, half-spacing fringes appear by the interference of simultaneously reflected waves. The half-spacing fringes do not move laterally by defocusing. Therefore, the energy spread of electrons has no blurring effect on the fringes, in the first order approximation. In the second order approximation, however, illumination angle 2β affects the contrast of the half-spacing fringes, coupling with defocusing width $\overline{\Delta f}$. The decrease of contrast[9] is also calculated to be

$$\frac{1}{\overline{\Delta f}}\int_{-\overline{\Delta f}/2}^{\overline{\Delta f}/2}\left\{\sin\left(\frac{4\pi\beta\Delta f}{d}\right)\Big/\frac{4\pi\beta\Delta f}{d}\right\}d(\Delta f).$$

It is also shown by curves (b) in Fig. 11, in both cases of $\beta=1\times10^{-3}$ rad and $\beta=5\times10^{-5}$ rad. In actual, the energy spread of the beam makes the contrast of the half-spacing fringes lower if three-wave interference is taken into consideration.

In the conventional electron microscope, β is about 1×10^{-3} rad, while β is as small as 5×10^{-5} rad in the field emission electron microscope. In addition to this effect, the narrow energy spread of electron beam makes the contrast of the fringes further better. With the field emission electron microscope, the contrast of half-spacing fringes is hardly decreased even if 0.5 Å lattice spacing is observed. Based on the above-mentioned consideration for improving the lattice resolution, lattice fringes were observed with the field emission electron microscope. However, there was a difficulty that the intensities of simultaneous Bragg-reflections diminish with the smaller lattice spacing. Intensities of simultaneous Bragg-reflections by three-wave approximation are calculated from the equation (33) in reference 11. The results are shown for gold and nickel in Fig. 13.

To observe half-spacing lattice fringes of {220} planes, the optimum thicknesses for the largest reflected intensities are 40 Å for gold and 35 Å for nickel, these intensities being 13% and 4% of incident electrons, respectively. The value of the optimum thickness for gold is larger than that for nickel, which

tendency is reversed in magnitude, compared with the case of two-wave approximation. This is due to the fact that incident electrons, parallel to lattice plane, are deviated from Bragg-condition and so the extinction distance becomes smaller, especially in the case of the small lattice spacing.

Lattice frings of the ⟨001⟩-oriented gold film taken with the field emission electron microscope are shown in Fig. 14. Half-spacing fringes of gold {220} planes are observed. The half spacing is equal to 0.72 Å, which was also taken by Sieber *et al.*[12] with special imaging technique. Furthermore, lattice fringes of the ⟨111⟩-oriented nickel film are given in Fig. 15. Half-spacing frings of {220} planes ($1/2\ d_{220}=0.62$ Å) are observed,[13] in addition to normal lattice fringes ($d_{220}=$ 1.2 Å). This is the smallest spacing fringes that have been ever taken.

In the same figure, the fringes with 0.72 Å spacing are also observed. They are due to the interference between two {220} reflected waves.

CONCLUSION

A field emission electron microscope has newly been developed. Both the gun and illuminating system were designed so as to obtain a highly stable electron beam with high brightness.

Several experiments were made to show the high performance of this microscope. The electron beam was stably obtained, whose brightness was 100 times larger than that of the conventional thermionic electron beam. This feature was successfully exemplified by the experimental results that 300 Fresnel fringes were taken with only 4 s and 3,000 bi-prism fringes were taken with 30 s. The decrease of energy spread of the electron beam made the effect of chromatic aberration considerably smaller in lattice imaging. In

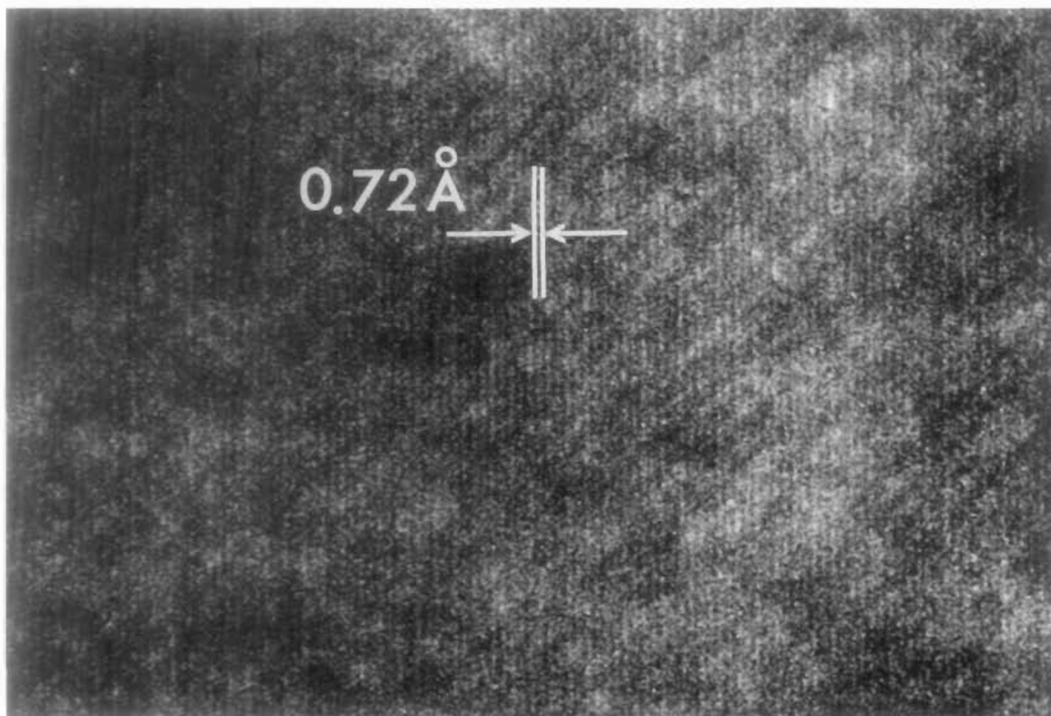

Fig. 14. Half-spacing fringes of gold {220} planes. The spacing of 0.72 Å is resolved, which was also observed by Sieber *et al.* with special imaging technique.[12]

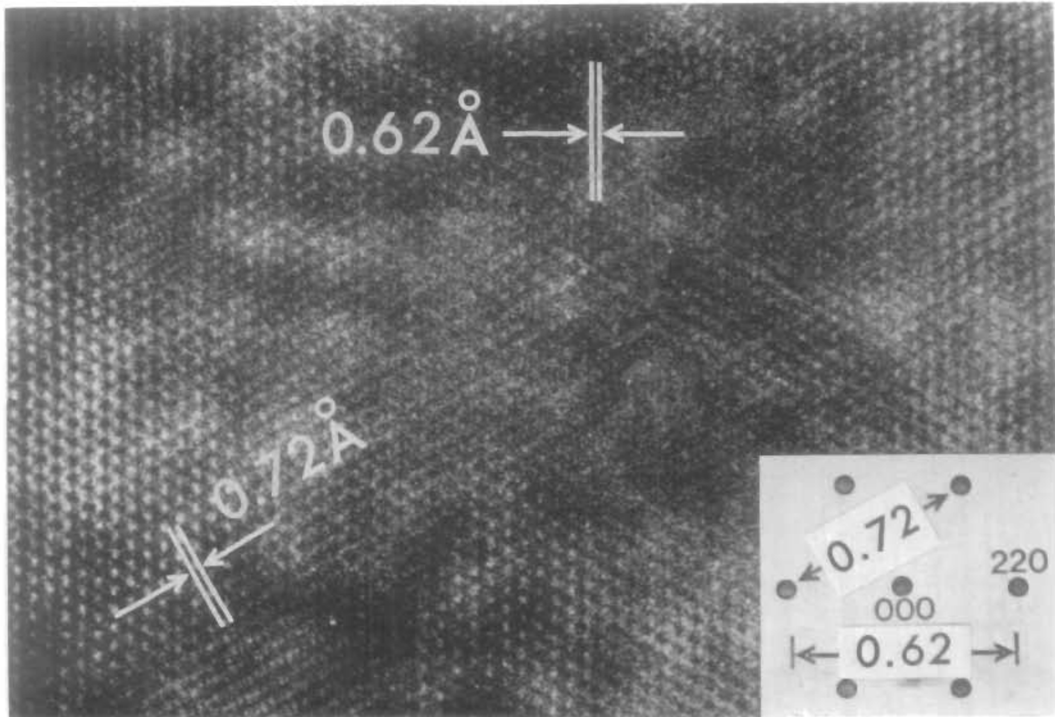

Fig. 15. Half-spacing fringes of nickel {220} planes. The spacing of 0.62 Å is resolved, which is the smallest structure that have ever been observed in electron microscopes.

actual, the half-spacing fringes of nickel {220} planes ($1/2\ d_{220}=0.62$ Å) were observed for the first time.

REFERENCES

1) Koops, H.: Proc. Int. Congr. Electron Microsc., 1978, Vol. 3, p. 185
2) Tonomura, A., Fukuhara, A., Komoda, T. and Watanabe, H.: *Jap. J. Appl. Phys.*, **7**, 259 (1968)
3) Möllenstedt, G. and Wahl, H.: *Naturwissenschaften*, **55**, 340 (1968)
4) Tomita, H., Matsuda, T. and Komoda, T.: *Jap. J. Appl. Phys.*, **9**, 719 (1970)
5) Möllenstedt, G. and Dücker, H.: *Naturwissenschaften*, **42**, 41 (1954)
6) Hibi, T. and Takahashi, S.: *J. Electron Microsc.*, **12**, 129 (1963)
7) Yada, K., Shibata, K. and Hibi, T.: *J. Electron Microsc.*, **22**, 223 (1973)
8) Tonomura, A., Matsuda, T. and Komoda, T.: *Jap. J. Appl. Phys.*, **17**, 1137 (1978)
9) Komoda, T.: Doctor thesis (Nagoya Univ., 1974).
10) Yada, K. and Hibi, T.: *J. Electron Microsc.*, **18**, 266 (1969)
11) Fukuhara, A.: J. Phys. Soc. Japan **21**, 2645 (1966)
12) Sieber, P. and Tonar, K.: *Optik*, **42**, 375 (1975)
13) Matsuda, T., Tonomura, A. and Komoda, T.: *Jap. J. Appl. Phys.*, **17**, 2073 (1978)